Defense Technical Information Center
Compilation Part Notice

ADP012586

TITLE: Successes and Predictions of a Pseudopotential Approach in Anion-Mixed Nitrides

DISTRIBUTION: Approved for public release, distribution unlimited

This paper is part of the following report:

TITLE: Progress in Semiconductor Materials for Optoelectronic Applications Symposium held in Boston, Massachusetts on November 26-29, 2001.

To order the complete compilation report, use: ADA405047

The component part is provided here to allow users access to individually authored sections of proceedings, annals, symposia, etc. However, the component should be considered within the context of the overall compilation report and not as a stand-alone technical report.

The following component part numbers comprise the compilation report:
ADP012585 thru ADP012685

Successes and Predictions of A Pseudopotential Approach in Anion-Mixed Nitrides

L. Bellaiche[1], A. Al-Yacoub[1], N.A. Modine[2] and E.D. Jones[2]
[1]Physics Department, University of Arkansas, Fayetteville, Arkansas 72701, USA
[2]Sandia National Laboratories, Albuquerque, New Mexico 87185, USA

ABSTRACT

The construction and the parameters of a new-strain dependent empirical pseudopotentials method are described and provided, respectively. This method is shown to reproduce with a very high accuracy some observed unusual properties in various complex anion-mixed nitride alloys. This method is also used to predict and understand anomalous effects that remain to be experimentally discovered in $Ga_{1-y}In_yAs_{1-x}N_x$ quaternaries and $GaAs_{0.5-x}P_{0.5-x}N_{2x}$ solid solutions.

INTRODUCTION

Anion-mixed nitride alloys exhibit very unusual properties. Examples of such anomalies are a large decrease of the band-gap when slightly increasing the nitrogen compositions [1-5] and a non-linear pressure behavior of the band-gap and exciton reduced masses in $GaAs_{1-x}N_x$ and $Ga_{1-y}In_yAs_{1-x}N_x$ [6-10]. Other examples include the strong dependency of the optical bowing coefficient [3,4], of the interband transition intensities [11] and of the effective electronic mass with nitrogen composition [12]. Other unusual features are the huge dependency of their optical and electronic properties with nitrogen atomic arrangement [13-15], as well as, the appearance of nitrogen impurity levels near the band edges in the dilute nitrogen impurity limit of $Ga_{1-y}In_yAs_{1-x}P_zN_{x+z}$ solid solutions [16-18]. Many recent studies have proposed rather different mechanisms for the microscopic effects responsible for these anomalies [3,6-9,18-21]. One possible reason for the present lack of consensus among researchers is the unprecedented difficulty of theoretically mimicking the properties of these alloys. As a matter of fact, some approximations, such as the virtual crystal approximation (VCA) [22], that can yield predictions in good agreement with measurements for conventional III-V alloys [11] are no longer valid in III-V-N solid solutions [11,23]. Similarly, the accurate description of various phenomena in anion-mixed nitride alloys requires the use of supercells that are too large to be handled by conventional first-principles calculations [18]. One computational alternative to the VCA and first-principles approaches is the so-called empirical pseudopotentials method (EPM). However, the accuracy provided by this approach strongly depends on the analytical form and on the parameters used to derive the pseudopotentials, which explains why different EPM can lead to quite different quantitative properties [3,9,10,18]. The goals of this article are (i) to describe in detail a new empirical pseudopotential method, (ii) to demonstrate that this method yields predictions in excellent agreement with measurements for various properties in complex anion-mixed nitride alloys, and (iii) to use this method to predict and understand effects that still remain to be experimentally discovered in III-V-N systems.

METHODS

Large relaxed supercells

To model a zinc-blende alloy, we use N x N x N conventional cubic cells, where the integer N can range from 4 to 8 --- which corresponds to a number of atoms varying from 512 to 4096. For *random* solid solutions, the atoms are randomly distributed on their sublattice sites, while the atoms in *ordered* alloys are located as consistent with the atomic ordering.

The valence force field (VFF) approach [24,25] is then used to predict the relaxed atomic positions corresponding to the minimum strain energy. Specifically, we use the bond-stretching (α) and bond-bending (β) of Ref. [26] for GaN (α=96.30 N/m and β=14.80 N/m) and InN (α=79.20 N/m and β=7.10 N/m), and of Ref. [25] for GaAs (α=41.19 N/m and β=8.95 N/m), InAs (α=35.18 N/m and β=5.50 N/m), GaP (α=47.32 N/m and β=10.44 N/m) and InP (α=43.04 N/m and β=6.24 N/m) in these VFF calculations. Reference[3] demonstrates that the VFF approach yields a good agreement with first-principles results for the internal atomic coordinates of anion-mixed nitride alloys.

Strain-dependent empirical pseudopotentials

Having obtained a relaxed configuration of a large, periodic unit cell, we compute its band structure by using the strain-dependent empirical pseudopotential approach proposed in Ref. [10]. The crystal potential V(r) is written as a superposition of atomic pseudopotentials v_γ (**r**), where γ= Ga, In, N, P or As .

For the As, P or N *anions* , the Fourier transform of v_γ (**r**) is given by:

$$v_\gamma (q) = [\Omega_\gamma \Sigma_m a_{m\gamma} \exp(-b_{m\gamma} (q - c_{m\gamma})^2)] \quad , \tag{1}$$

where the m integers range from 1 to 4.

For the Ga or In cations, the analytical expression of v_γ (q) becomes more complicated:

$$v_\gamma (q) = \Sigma_A [\Omega_{\gamma(A)} \Sigma_m a_{m\gamma(A)} \exp(-b_{m\gamma(A)} (q - c_{m\gamma(A)})^2)] [n(\gamma\text{-}A)+n(\gamma\text{-}A) d_{ma}(\gamma(A)) Tr(\varepsilon_{ma})$$
$$+ (x_N f_{mi}(\gamma(A)) + g_{mi}(\gamma(A))) \Sigma_j Tr(\varepsilon_{mi}(\gamma\text{-}A_j))] \quad , \tag{2}$$

where the first sum runs over the different *kinds* of anions (e.g., A = As, P and N) nearest neighbors of the γ cation in the alloy, 'γ (A)' denotes a γ cation bonding with an anion A and n(γ-A) is the number of type A anions that are nearest neighbors of this γ cation. Furthermore, Tr denotes the trace operator and ε_{ma} is the *macroscopic* strain induced by an external stress, e.g., applying a hydrostatic pressure P to the alloy leads to:

$Tr(\varepsilon_{ma}) = 3 \ (a(P)-a(P=0))/a(P=0)$, where a(P) and a(P=0) are the alloy lattice constants associated with the pressure P and at equilibrium, respectively. x_N is the nitrogen composition in the alloy, and the last sum runs over the different j atoms of type A which are nearest neighbors of the γ cation. $\varepsilon_{mi}(\gamma-A_j)$ is the *microscopic* strain induced by alloying, e.g., for an alloy at its equilibrium lattice constant, we have:

$$Tr(\ \varepsilon_{mi}(\gamma-A_j) \ ) = [\ (\ | \ R_x(\gamma-A_j) \ | - d_0(\gamma A) \ ) \ ] / d_0 \ (\gamma A)] + [\ (\ | \ R_y(\gamma-A_j) \ | - d_0(\gamma A) \ ) \ ] / d_0 \ (\gamma A)] + [\ (\ | \ R_z(\gamma-A_j) \ | - d_0(\gamma A) \ )/d_0 \ (\gamma A)] \quad ,$$
$$(3)$$

where $| \ R_x(\gamma-A_j) \ |$ (respectively, $| \ R_y(\gamma-A_j) |$ and $| \ R_z(\gamma-A_j) \ |$) is the absolute value of the x- (respectively, y- and z-) component of the vector position joining the γ atom to the A_j anion in the alloy. $d_0(\gamma A)$ is the corresponding equilibrium Cartesian component in the pure zinc-blende γA binary.

One can note that, unlike in Refs [3,9,18], the contribution of both the macroscopic and the microscopic strain is taken into account for the generation of the pseudopotentials.

The strain-unrelated parameters of Eqs. (1) and (2), i.e. the Ω_γ, $a_{m\gamma}$, $b_{m\gamma}$ and $c_{m\gamma}$ coefficients, are fitted carefully to *ab-initio* band structures and to the experimental band-gaps of the corresponding γA binaries at their equilibrium lattice constants a_0 (with a_0 =8.523, 10.300, 10.6826, 9.4108, 11.0105 and 11.444 Bohr for GaN, GaP, GaAs, InN, InP and InAs, respectively), and are given in Table I and Table II, respectively. Some of these coefficients were already given in Ref. [3] and references therein.

Table I. Strain-unrelated empirical pseudopotentials parameters for the different anions.

Atom γ	Ω_γ (a.u.)^3	m	$a_{m\gamma}$ (Ry)	$b_{m\gamma}$ (a.u.)$^{-1}$	$c_{m\gamma}$ (a.u.)^2
N	75.0	1	-0.22628191	1.816012550	0.000000000
		2	0.02083001	13.51921051	2.628521803
		3	0.23728104	0.909593411	1.555913001
		4	-0.92682699	0.918842363	0.851766355
P	139.2	1	-1.02821000	0.870327000	0.000000000
		2	0.01217600	5.811450000	2.400080000
		3	-0.04943100	3.186790000	0.889644000
		4	0.11769000	0.470922000	1.028360000
As	145.2	1	-1.05821000	0.959327000	0.000000000
		2	-0.00217627	6.531450000	2.468080000
		3	-0.04343120	2.946790000	0.851644000
		4	0.10569000	0.820922000	1.224360000

Table II. Strain-unrelated empirical pseudopotentials parameters for the different cations.

Atom γ (A)	$\Omega_{\gamma(A)}$ (a.u.)^3	m	$a_{m\gamma(A)}$ (Ry)	$b_{m\gamma(A)}$ (a.u)$^{-1}$	$c_{m\gamma(A)}$ (a.u.)^2
Ga(N) =	131.4	1	-1.24498000	1.527480000	0.000000000
Ga(P) =		2	0.03665200	0.959082000	2.097820000
Ga(As)		3	0.04643600	0.574047000	2.019350000
		4	-0.01333800	11.27080000	2.935810000
In(N)	131.8	1	-1.46039000	2.152539077	0.000000000
		2	0.04155672	0.567806063	2.455282992
		3	0.06009332	0.148458154	2.251294168
		4	-0.01593695	13.75237193	2.728137391
In(P)	131.4	1	-1.45986104	1.738812400	0.000000000
		2	0.05977844	0.537256952	1.788116476
		3	0.04656102	0.967274227	2.926947028
		4	-0.02482974	3.509813326	3.447074186
In(As)	131.4	1	-1.44017756	1.729912675	0.000000000
		2	0.05814899	0.503547419	1.790927031
		3	0.04869021	1.177591464	3.265606034
		4	-0.01632399	4.001886743	4.019772670

The coefficients $d_{ma}(\gamma(A))$ in Eq.(2) are fitted to reproduce the local density approximations (LDA) deformations potentials of both the valence band maximum and conduction band minimum of the pure zinc-blende γA *binary* [27]. On the other hand, the parameters $f_{mi}(\gamma(A))$ and $g_{mi}(\gamma(A))$ are fitted to reproduce *alloy* quantities, namely the experimental bowing coefficient of $Ga(As_{1-x}N_x)$ with x=0.004 (see Refs [4-5] and references therein), $In(P_{1-x}N_x)$ with x=0.004 [28] and $(Ga_{1-y}In_y)N$ with y =0.1 [29-30], as well as the arsenic-impurity level observed in the GaN:As system [31]. The parameters that are strain-related and that enter Eq(2) are given in Table III.

Table III. Strain-related empirical pseudopotentials parameters for the different cations.

Cation γ (A)	d_{ma}	f_{mi}	g_{mi}
Ga(N)	0.1353	-0.4233	0.5817
Ga(P)	0.1870	0.0000	0.0000
Ga(As)	0.1870	0.0000	0.0000
In(N)	0.1615	-1.1800	1.2800
In(P)	0.2000	0.0000	0.0000
In(As)	0.2000	0.0000	0.0000

Plane-wave expansion and folded spectrum method

The electronic eigenfunctions of the Hamiltonian given by the sum of the kinetic energy and the empirical pseudopotentials are developed in a plane-wave basis with a kinetic energy cutoff denoted by G_{max}. Due to the large difference in equilibrium lattice constant

between the end-member binaries, G_{max} is chosen to be dependent on the volume of the system under investigation. More precisely, G_{max} should correspond to 59 plane waves at the Γ point per 2-atoms zinc-blende cell. As a result, systems exhibiting an equilibrium volume per 2 atoms identical to the one of pure GaAs are associated with a G_{max} of 5 Ry while the kinetic energy cutoff is 7.87 Ry in compounds having the equilibrium volume per 2 atoms of zinc-blende GaN. Note that the parameters displayed in Tables I-III were fitted using this volume-dependent kinetic energy cutoff.

The eigenfunctions and eigenvalues of the Schrodinger equation for the large supercells are determined by using the so-called folded spectrum method [32]. This numerical technique is a method scaling linearly with the number of atoms in the supercell, and producing single-particle eigensolutions in a given energy window.

RESULTS

Accuracy of the strain-dependent empirical pseudopotentials

In this section, we will demonstrate the accuracy provided by our numerical scheme. With the exception of the band-gap of $GaAs_{1-x}N_x$ with x=0.4% and epitaxially grown on GaAs, all the results to be shown were not included in the fitting of the EPM parameters.

The first test is displayed in Table IV and consists in comparing our calculations with low-temperature measurements for the band-gaps of *disordered* $Ga_{1-y}In_yAs_{1-x}N_x$ *quaternaries* that are perfectly lattice-matched to either a GaAs or InP substrate. Because of this perfect lattice-match, the microscopic strain ε_{mi} is the only strain turned on in the generation of the pseudopotentials in Eq. (2). Table IV indeed reveals the high accuracy offered by the strain-dependent EPM described above. In particular, one can notice that the difference between predictions and measurements does not exceed 0.03 eV for a range of band-gap as large as 0.9 eV.

Table IV. Comparison between our predictions and experiments for the band-gaps of $Ga_{1-y}In_yAs_{1-x}N_x$ quaternaries perfectly lattice-matched to a GaAs [*] or InP [**] substrate.

(y, x) compositions of $Ga_{1-y}In_yAs_{1-x}N_x$	Theoretical band-gap (eV)	Experimental band-gap (eV)
(0.00, 0.000) [*]	1.52	1.52 (Ref. 7)
(0.07, 0.022) [*]	1.18	1.15 (Ref. 7)
(0.53, 0.000) [**]	0.82	0.82 (Ref. 33)
(0.56, 0.010) [**]	0.73	0.70 (Ref. 33)
(0.59, 0.019) [**]	0.65	0.65 (Ref. 33)

The second test is indicated in Fig. 1, which displays the comparison between our predictions and available experimental data for the compositional behavior of the band-gap of *random* $GaAs_{1-x}N_x$ *ternaries* epitaxially grown on a GaAs substrate. In such a case, both the macroscopic ε_{ma} and microscopic ε_{mi} strains appearing in Eq (2) are activated because of the epitaxial conditions and alloying, respectively. Figure 1 also

shows the predictions of the empirical pseudopotentials when all the strain-related coefficients of Table III have been turned off. In this figure, our calculated T=0K band-gaps have been shifted downward, by using the temperature-dependency measured in Ref. [34], to compare our predictions with the recent *room-temperature* experiments of Refs. [5,35,36]. Figure 1 reveals an excellent agreement between the present strain-dependent EPM theory and measurements, and clearly demonstrates that the contribution of both the macroscopic and the microscopic strains to the empirical pseudopotentials drastically improves the accuracy of the calculations for anion-mixed nitrogen systems.
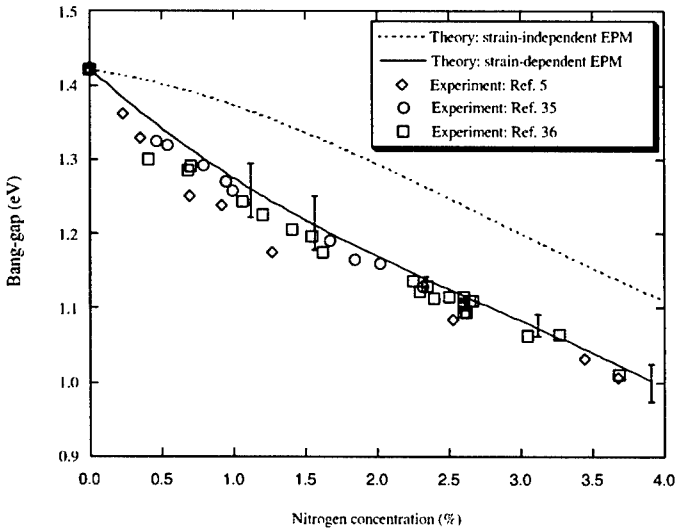
Figure 1. Comparison between our predictions, using empirical pseudopotentials methods (EPM), and experiments for the room-temperature band-gaps of $GaAs_{1-x}N_x$ alloys epitaxially grown on a GaAs substrate. Theoretical error bars are also indicated.

The result of the third test is reported in Figure 2, which shows our predictions and a low-temperature measurement [7] for the pressure-dependency of the band-gap in the random $Ga_{1-y}In_yAs_{1-x}N_x$ quaternary, with (y,x)=(0.07, 0.0023). Here, both macroscopic and microscopic strains are taken into account in Eq (2) because of the pressure and alloying, respectively. The calculations are corrected by multiplying the pressure-induced alloy band-gap shift by a constant number --- equal to 1.2885. This number is fitted to exactly reproduce the experimental hydrostatic deformation potential in zinc-blende GaAs. Our numerical results are once again in good agreement with measurements. In particular, one

can notice that the unusual non-linear pressure behavior of the band-gap is rather well reproduced up to 60Kbar.

The next step consists in identifying the energy of the nitrogen impurity level which is usually denoted $a_1(N)$ [9,18,21] and which is *resonant* inside the conduction band of nitrogen-dilute $GaAs_{1-x}N_x$ alloys. Such identification is realized by interpolating our results for one nitrogen atom inside a 1728 atoms-cell and inside a 4096 atoms-cell.
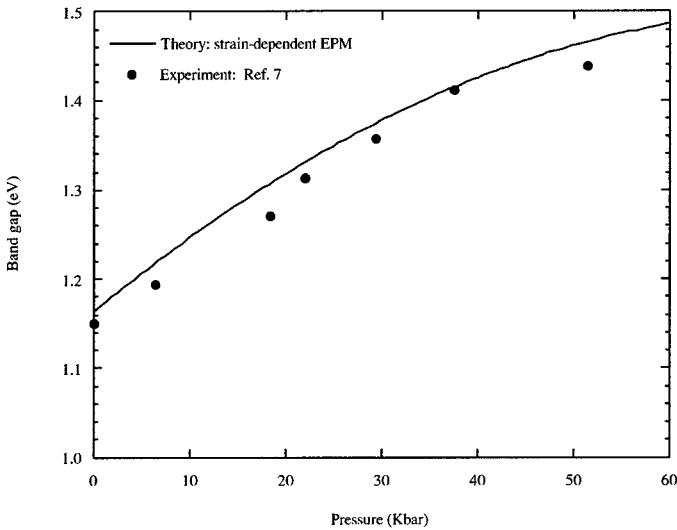

Figure 2. Comparison between our strain-dependent empirical pseudopotentials calculations and the experiment of Ref. [7] for the pressure-behavior of the band-gap in $Ga_{1-y}In_yAs_{1-x}N_x$ quaternaries with (y,x)=(0.07, 0.023).

$a_1(N)$ is found to be located 250 meV above the (CBM) Γ_{1c} level (or equivalently, 36 meV below the L_{1c} state) of GaAs, which is in excellent agreement with the experimental estimations of 300 meV above Γ_{1c} [37] and 30 meV below L_{1c} [38], as well as with the LDA calculations of Ref. [21] yielding 280 meV above Γ_{1c}.

The last test of this subsection is the prediction of the energy of the deep-gap impurity level occurring when adding a small amount of nitrogen to the $Ga(As_{0.5}P_{0.5})$ alloy. This

energy is found by linearly interpolating up to a null nitrogen composition the impurity levels predicted by our strain-dependent EPM for a nitrogen composition of 0.00116 and of 0.002. Such interpolation yields a nitrogen-impurity level located 115 meV below the conduction band-minimum of $Ga(As_{0.5}P_{0.5})$ alloy, which is in good agreement with the experimental value of 130 meV [16].

Prediction of anomalies in anion-mixed nitride alloys

The aim of this section is to review and to provide an explanation for the anomalies that were recently predicted to occur in anion-mixed nitrides, by using the present EPM [10,14,17]. Most of these anomalies remain to be experimentally discovered.

Predictions for (Ga,In)(As,N) alloys:

Ref. [10] predicted that the band-gap of the random $Ga_{1-y}In_yAs_{1-x}N_x$ quaternaries lattice-matched to a GaAs or InP substrate strongly decreases when increasing the nitrogen composition (Note that this increase of nitrogen concentration was accompanied by a simultaneous increase in the indium composition in order to keep a perfect lattice-match to the substrate). As a result, the band-gap of both lattice-matched $Ga_{1-y}In_yAs_{1-x}N_x$ systems crosses important technological spectral regions, namely the ones desired for optoelectonics, for solar cell applications, for designing new infrared devices and even for generating terahertz wavelengths [10]. Moreover, Ref. [10] further indicated that the band-gaps of both lattice-matched quaternaries even close for large enough nitrogen composition (namely, for x=0.12 for the InP-lattice matched quaternaries versus x=0.20 for the $Ga_{1-y}In_yAs_{1-x}N_x$ alloys lattice matched to GaAs). In other words, these strain-dependent EPM calculations predict that it is possible to create a metallic system by mixing four semiconductors (namely, GaAs, InAs, GaN and InN)! They also demonstrate that the common empirical rule that there is a one-by-one correspondence between the value of the lattice constant and the value of the band-gap in semiconductors is completely invalid in anion-mixed nitride alloys.

Another recent article focused on the effect of *atomic ordering* on optical and electronic properties of the GaAs-lattice matched $Ga_{1-y}In_yAs_{1-x}N_x$ solid solutions with a indium and nitrogen composition of 5% and 1.6%, respectively [14]. Three different samples were generated. The first configuration mimicks the *random* $Ga_{0.95}In_{0.05}As_{0.984}N_{0.016}$ system. The second selected sample corresponds to the formation of one-dimensional nitrogen chains along the [001] cubic direction, such as each nitrogen atom has two other nitrogen

Table V. Band-gap of differently atomically-ordered $Ga_{0.95}In_{0.05}As_{0.984}N_{0.016}$ alloys.

$Ga_{0.95}In_{0.05}As_{0.984}N_{0.016}$ System	Band-gap (eV)
Random	1.27
With nitrogen chains formed along [100]	1.33
With nitrogen chains formed along [110]	1.12

atoms as *second neighbors* in the anion sublattice. The last chosen configuration also exhibits one-dimensional nitrogen chains but for which each nitrogen atom has now two other nitrogen atoms as *fourth neighbors* in the anion sublattice. The resulting direction of this chain is thus along the [110] direction. This peculiar atomic ordering was chosen because the nitrogen chains can be perceived as a bridge between the case of N-N pairs in GaAs and the case of more concentrated nitrogen alloys. Moreover, we decided to specifically choose the [100] and [110] directions as directions for the one-dimensional nitrogen chains because the formation of second neighbor N-N pair in GaAs is known to slightly increase the band-gap with respect to random Ga(As,N) alloys, while fourth neighbor N-N pair significantly decreases that band-gap [13]. We thus expected that the one-dimensional nitrogen chains formed along the [100] direction may affect the properties of (Ga,In)(As,N) quaternaries in an opposite way (with respect to the case of the disordered alloy) than the [110] nitrogen chains. Table V indeed reports that the band-gap of the ordered material exhibiting nitrogen chains arranged along the [110] direction is *smaller* (by 0.15 eV) than the band-gap of the random alloy, while the sample with one-dimensional nitrogen chains formed along the [100] direction has a band-gap *larger* by 0.06 eV than the band-gap of the disordered alloy. This variation of the band-gap with atomic ordering is quite remarkable, especially when realizing that the nitrogen composition of these alloys is as small as 1.6%.

Another finding reported in Ref. [14] is the correlation between the value of the band-gaps displayed in Table V and the wavefunction localization of the conduction band-minimum (CBM) in these alloys. In the calculations, smaller band-gaps were found to correspond to stronger localization of the alloy CBM electronic state around the nitrogen atoms.

A simple model was further proposed in Ref. [14] to provide a *qualitative* explanation for the anomalies indicated above. This model is based on the perturbation theory at the second-order in energy (and equivalently to the first-order in wavefunction), i.e. one can write the CBM energy E_{CBM} of the $Ga_{1-y}In_yAs_{1-x}N_x$ alloy as:

$$E_{CBM} = E_{\Gamma,c} + <\Phi_{\Gamma,c}|\, \delta V\,|\Phi_{T,c}> + \Sigma_k\, (\, <\Phi_{\Gamma,c}|\, \delta V\,|\Phi_{k,c}>^2 /\, (E_{\Gamma,c} - E_{k,c})\,)\ , \qquad (4)$$

while the alloy CBM wavefunction Ψ_{CBM} is given by

$$\Psi_{CBM} = \alpha\, [\Phi_{\Gamma,c} + \Sigma_k\, \Phi_{k,c}\, (|<\Phi_{\Gamma,c}|\, \delta V\,|\Phi_{k,c}>|\, /\, (E_{\Gamma,c} - E_{k,c})\,)\,]\ , \qquad (5)$$

where $\Phi_{\Gamma,c}$ (respectively, $E_{\Gamma,c}$) and $\Phi_{k,c}$ (respectively, $E_{k,c}$) are the conduction states (respectively, energies) of the appropriate *nitrogen-lacking system*, at Γ and at off-centers k-points, respectively. The nitrogen-lacking system is zinc-blende GaAs in the case of the $Ga_{1-y}In_yAs_{1-x}N_x$ alloys lattice-matched to GaAs while it is the $Ga_{0.47}In_{0.53}As$ alloy for the InP-lattice-matched $Ga_{1-y}In_yAs_{1-x}N_x$ solid solutions. Note that the difference in energy $E_{\Gamma,c} - E_{k,c}$ is negative for any off-center k-points since the CBM of both GaAs and $Ga_{0.47}In_{0.53}As$ materials occurs at the Γ point. δV is the difference of potentials between the nitride quaternaries and the nitrogen-lacking system, while α is a normalization coefficient. Ref. [14] proposes that the large band-gap redshift occurring when inserting

nitrogen atoms into the $Ga_{1-y}In_yAs$ alloy is imputable to (at least) two different effects. First, the first-order perturbative term in Eq. (4) (i.e., the $<\Phi_{\Gamma,c} | \delta V |\Phi_{\Gamma,c}>$ element) strongly shifts the energy of the alloy CBM towards the energy of the alloy valence-band-maximum. We numerically found that this first effect contributes 60% of the decrease of the band-gap of the random $Ga_{0.95}In_{0.05}As_{0.984}N_{0.016}$ alloy with respect to the band-gap of pure zinc-blende GaAs. Such a first-order term, which only involves the Γ point and the nitrogen-induced change in potential, has been overlooked in the previous studies, to our knowledge. The second effect is derived from the second-order term of Eq (4) and is therefore a manifestation of nitrogen-induced quantum coupling between different electronic states of the nitrogen-lacking system. In agreement with some recent studies [7,9,21], the most quantitatively important quantum couplings were found to occur between the Γ and L-points and between the Γ and X-points [10,14]. (Note that the effects proposed in Refs [6,9,20,21] and involving *nitrogen impurity levels* may also play a role in the decrease of the band-gap, especially for very small nitrogen concentrations). Interestingly, atomic ordering in $Ga_{1-y}In_yAs_{1-x}N_x$ alloys does not affect the first-order perturbative term of Eq (4) but rather significantly changes the $<\Phi_{\Gamma,c} | \delta V |\Phi_{k,c}>$ electronic coupling elements. In particular, it was found that some specific electronic coupling can be *turned on and off* with atomic arrangement. As it can be seen by looking at Eq. (5), the atomic-ordering dependency of $<\Phi_{\Gamma,c} | \delta V |\Phi_{k,c}>$ also provides a ``natural'' explanation for the predicted change of localization of the alloy CBM state with nitrogen atomic arrangement. Note that a recent study [15], also using the present strain-dependent empirical pseudopotential technique, demonstrated that short-range atomic ordering in $Ga_{1-y}In_yAs_{1-x}N_x$ affects the coupling between the Γ and L-points, which is consistent with our findings.

Predictions for Ga(As,P,N) alloys:

$GaAs_{0.5-x}P_{0.5-x}N_{2x}$ alloy differentiates itself from the $Ga_{1-y}In_yAs_{1-x}N_x$ solid solution by two main features. First of all, it contains three different anions rather than two, which constitutes an additional computational difficulty. Secondly and more importantly, inserting a very small amount of nitrogen into $GaAs_{0.5}P_{0.5}$ leads to a deep impurity level located *below* the conduction band-minimum of $GaAs_{0.5}P_{0.5}$, i.e. the lowest unoccupied state of dilute $GaAs_{0.5-x}P_{0.5-x}N_{2x}$ is localized around the nitrogen atoms [16]. On the other hand, the nitrogen impurity level occurring in $Ga_{1-y}In_yAs_{1-x}N_x$ alloy, with very small x, is resonant *inside* the conduction band of $Ga_{1-y}In_yAs$ [16]. The aim of Ref. [17] was to follow and understand the evolution of the character and energy position of the lowest unoccupied state in $GaAs_{0.5-x}P_{0.5-x}N_{2x}$ when incorporating more and more nitrogen atoms. It was found that the evolution of this state is highly unusual. More precisely, as nitrogen is added, this lowest unoccupied state gradually evolves from an impurity localized level to a delocalized Bloch-like state. This evolution occurs over a very narrow nitrogen composition window centered around 0.4%. In other words, adding a very small amount of nitrogen drastically changes the character of the lowest unoccupied state of $GaAs_{0.5-x}P_{0.5-x}N_{2x}$. This change of character is due to two different and simultaneous quantum-mechanical processes. The first process is an *anticrossing*

between the nitrogen impurity level existing in the dilute alloy limit (for which x goes to zero) and the Γ conduction state of the nitrogen-lacking $GaAs_{0.5}P_{0.5}$ system. The second process is a repulsion between the deep-gap nitrogen levels that results in the formation of a *nitrogen subband*. One direct consequence of these double processes is that the difference in energy between the lowest unoccupied and the highest occupied levels of $GaAs_{0.5-x}P_{0.5-x}N_{2x}$ strongly decreases when increasing the nitrogen concentration. As a matter of fact, incorporating only 1% of nitrogen into $GaAs_{0.5}P_{0.5}$ leads to a difference in energy of 1.8 eV, i.e. around 300 meV smaller than the band-gap of $GaAs_{0.5}P_{0.5}$.

CONCLUSIONS

This article demonstrates that many highly unusual properties of various anion-mixed nitride alloys (including $GaAs_{1-x}N_x$ ternaries, $Ga_{1-y}In_yAs_{1-x}N_x$ quaternaries and systems exhibiting three different anions such as $GaAs_{0.5-x}P_{0.5-x}N_{2x}$) can be accurately reproduced by using a new strain-dependent empirical pseudopotential method. The details of the construction of this method, as well as its parameters, are provided for the first time. Finally, this new method was used to predict and understand other anomalies, such as (i) a closing of the band-gap in $Ga_{1-y}In_yAs_{1-x}N_x$ quaternaries lattice-matched to GaAs or InP substrate, (ii) a drastic change of character of the lowest unoccupied state of $GaAs_{0.5-x}P_{0.5-x}N_{2x}$ and (iii) the strong-dependency of anion-mixed nitrides' properties with the nitrogen atomic arrangement. These anomalies, which were qualitatively explained via some simple quantum mechanical effects, remain to be experimentally observed.

ACKNOWLEDGMENTS

REFERENCES

1. M. Weyers, M. Sato and H. Ando, *Jpn. J. Appl. Phys.* **31**, L853 (1992).
2. M. Kondow *et al*, *Jpn. J. Appl. Phys.* **33**, L1056 (1994).
3. L. Bellaiche, S-H. Wei and A. Zunger, *Phys. Rev. B* **54**, 17568 (1996).
4. W.G. Bi and C.W. Tu, *Appl. Phys. Lett.* **70**, 1608 (1997).
5. K. Uesugi, N. Morooka and I. Suemune, *Appl. Phys. Lett.* **74**, 1254 (1999).
6. W. Shan, W. Walukiewicz, J.W. Ager III, E. E. Haller, J.F. Geisz, D.J.Friedman, J.M. Olson and S.R. Kurtz , *Phys. Rev. Lett.* **82**, 1221 (1999).
7. E.D. Jones, N.A. Modine, A.A. Allerman, S.R. Kurtz, A.F. Wright, S.T. Tozer and X. Wei, *Phys. Rev. B.* **60**, 4430 (1999).
8. E.D. Jones, A.A. Allerman, S.R. Kurtz, N.A. Modine, K.K. Bajaj, S.T. Tozer and X. Wei, *Phys. Rev. B.* **62**, 7144 (2000); E.D. Jones *et al*, *Proc SPIE* **3621**, 52 (1999); E.D. Jones *et al*, *Proc SPIE* **3944**, 80 (2000).
9. T. Mattila, S.H.- Wei and A. Zunger *Phys. Rev. B.* **60**, R11245 (1999).

10. L. Bellaiche, *Appl. Phys. Lett.* **75**, 2578 (1999).
11. L. Bellaiche, S-H. Wei and A. Zunger, *Phys. Rev. B* **56**, 10233 (1997).
12. Y. Zhang, A. Mascarenhas, H.P. Xin and C.W. Tu, *Phys. Rev. B* **61**, 7479 (2000).
13. L. Bellaiche and A. Zunger, *Phys. Rev. B* **57**, 4425 (1998).
14. Al-Yacoub and L. Bellaiche, *Phys. Rev. B* **62**, 10847 (2000).
15. K. Kim and A. Zunger, *Phys. Rev. Lett.* **86**, 2609 (2001).
16. R.J. Nelson, in *Excitons*, edited by E.I. Rashba and M.D. Sturge, North-Holland Publishing company (1982).
17. L. Bellaiche, N.A. Modine and E.D. Jones, *Phys. Rev. B* **62**, 15311 (2000).
18. P.R.C. Kent and A. Zunger, *Phys. Rev. B* **64**, 115208 (2001); *Phys. Rev. Lett.* **86**, 2613 (1996).
19. S.-H. Wei and A. Zunger, *Phys. Rev. Lett.* **76**, 664 (1996).
20. Y. Zhang, A. Mascarenhas, H.P. Xin and C.W. Tu, *Phys. Rev. B* **63**, 161303 (2001).
21. L.-W. Wang, *Appl. Phys. Lett.* **78**, 1565 (2001).
22. J.A. Van Vechten, *Phys. Rev.* **182**, 891 (1969).
23. L. Bellaiche, S-H. Wei and A. Zunger, *Appl. Phys. Lett.* **70**, 3558 (1997).
24. P.N. Keating, *Phys. Rev.* **145**, 637 (1966).
25. R.M. Martin, *Phys. Rev. B* **1**, 4005 (1970).
26. K. Kim, W.R.L. Lambrecht and B. Segall, *Phys. Rev. B* **53**, 16310 (1996).
27. S.-H. Wei and A. Zunger, *Phys. Rev. B* **60**, 5404 (1999).
28. W.G. Bi and C.W. Tu, *J. Appl. Phys.* **80**, 1934 (1996).
29. C. Wetzel, T. Takeuchi, S. Yamaguchi, H. Katoh, H. Amano and I. Akasaki, *Appl. Phys. Lett.* **73**, 1994 (1998).
30. M.D. Cluskey, C.G. Van de Walle, C.P. Master, L.T. Romano, and N.M. Johnson, *Appl. Phys. Lett.* **72**, 2725 (1998).
31. J.I. Pankove and J.A. Hutchby, *J. Appl. Phys.* **47**, 5387 (1976).
32. L.W. Wang and A. Zunger, *J. Chem. Phys.* **100**, 2394 (1994).
33. M.R. Gokhale, J. Wei, H. Wang and S.R. Forrest, *Appl. Phys. Lett.* **74**, 1287 (1999).
34. K. Uesugi, I. Suemune, T. Hasegawa, T. Akutagawa and T. Nakamura, *Appl. Phys. Lett.* **76**, 1285 (2000).
35. L. Malikova, F.H. Pollack and R. Bhat, *J. Electron. Mater* **27**, 484 (1998).
36. P. Gilet, L. Grenouillet, P. Duvaut, P. Ballet, G. Rolland, C. Vannuffel and A. Million, *J. Vac. Sci. Technol. B.* **19**, 1422 (2001).
37. H.P. Hjalmarson, P. Vogl, D.J. Wolford and J.D. Dow, *Phys. Rev. Lett.* **44**, 810 (1980).
38. J.D. Perkins, A. Mascarenhas, Y. Zhang, J.F. Geisz, D.J. Friedman, J.M. Olson and S.R. Kurtz, *Phys. Rev. Lett.* **82**, 3312 (1999).